AN EXPERIMENTAL AND COMPUTATIONAL STUDY OF DIRECTIONAL SOLIDIFICATION IN TRANSPARENT MATERIALS

James E. Simpson[†], Henry C. de Groh III[‡] and Suresh V. Garimella[†]

[†]Mechanical Engineering Department
University of Wisconsin - Milwaukee
P.O. Box 784, Milwaukee, Wisconsin 53201

[‡]NASA Lewis Research Center
MS 105-1, Cleveland Ohio 44135

Abstract

An experimental and numerical study of the horizontal Bridgman growth of pure succinonitrile (SCN) and of a succinonitrile-1.0 mol.% acetone alloy (SCN-1.0 mol.% ACE) has been performed. Experiments at growth rates of 0, 2 and 40 μm/s were investigated. The solid/liquid interface was stable (non-dendritic and non-cellular); however, it was not flat. Rather, it was significantly distorted by the influence of convection in the melt and, for the growth cases, by the moving temperature boundary conditions along the ampoule. For the alloy, the interface was determined to be unstable at growth rates greater than 2.8 μm/s, but stable for the no-growth and 2 μm/s growth cases. When compared to the pure SCN interface, the alloy interface forms closer to the cold zone, indicating that the melting temperature has been suppressed by the addition of the alloying element. Two-dimensional computer simulations were performed for the no-growth case for both the pure and alloy materials. These simulations indicate that a primary longitudinal convective cell is formed in the melt. The maximum magnitude of velocity was calculated to be 1.515 mm/s for pure SCN and 1.724 mm/s for the alloy. The interface shape predicted by the computer simulation agrees well with the experimentally determined shape for the pure SCN case. In ongoing work, numerical simulations of the process during growth conditions are being performed.

Invited paper to Symp. On Fluid Flow Phenom. In Metals Processing, 1999 TMS Annual Meeting, San Diego, Feb., 1999.

Introduction

Increasingly, advanced materials used in the aerospace, automotive, optics and electronics fields require low levels of defects and high levels of solute uniformity. Directional solidification by the Bridgman process is widely used for synthesis of these high-quality materials. During Bridgman crystal growth, heat and mass transfer by both thermal and solutal gradient-driven convection and diffusion influence the shape of the solid/liquid interface and dopant segregation levels, and hence, directly determine the final crystal quality. Key process parameters include the applied furnace temperature distribution and rate of translation, ampoule properties and furnace orientation.

Experimental investigations of solidification processes which involve metallic melts are complicated by the opacity, reactivity and high temperatures of the melts. Accurate experimental determination of the interface shape and convection is difficult. A means of reducing the difficulty and achieving accuracy in solidification experiments is to use transparent materials that solidify in a manner analogous to metals. Experiments using such transparent metal analogs are widely reported in the literature [1, 2, 3]. Computer simulations are also employed to investigate solidification processes [4, 5, 6, 7]. Such computer models can be checked and enhanced by comparison with experimental results.

The aim of the current work is to perform a detailed experimental and numerical investigation of the Bridgman crystal growth process under terrestrial conditions. These results build on existing experiments performed under similar conditions [1]. Transparent metal analogs, namely pure succinonitrile (SCN) and a binary alloy of succinonitrile and 1.0 molar percent acetone (SCN-1.0 mol.% ACE), are employed as the phase-change materials. Interface shape data are obtained for both materials under no-growth and solidification conditions. The temperature field applied by the furnace is measured. In addition, video images of seed particles moving in the melt are employed to estimate convective velocities in the pure SCN sample under no-growth and solidification conditions. The experimentally determined thermal boundary conditions and interface shape are then used to perform and validate numerical simulations of the process. The results from these simulations agree well with the experiments in terms of the interface shape for the pure SCN case and elucidate the impact of melt convection on the Bridgman process.

Experimental Setup

The NASA-Lewis Transparent Directional Solidification Furnace (TDSF) is shown schematically in figure 1. The TDSF is a Bridgman-type furnace with two copper jackets separated by an air gap which acts as the gradient or adiabatic zone between the two jackets and also permits viewing of the glass ampoule which contains the phase change material. Constant-temperature circulating water baths provide the temperature set points for each jacket. The apparatus may be oriented in any direction; however, only the horizontal configuration is considered in this work.

The 150 mm long ampoules used are made of borosilicate glass with a square cross section. The ampoules are 8 mm on a side and have a wall thickness of approximately 1 mm. The thermal jackets have a 11 mm square hole running through their entire lengths into which the (smaller) ampoule is inserted. Accurate alignment and centering of the ampoule within the jackets is essential to obtaining repeatable results. For growth experiments, a servomotor with reducing gear translates the cooling jackets at a desired constant velocity (2 or 40 μm/s for the present work). The motor and indexer locate the jackets very accurately.

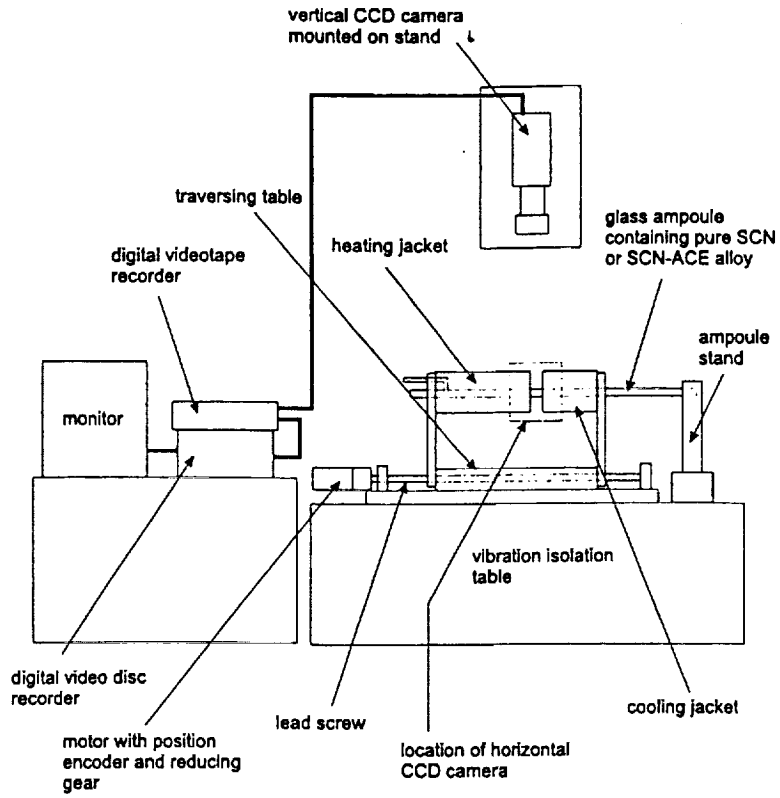

Figure 1: Schematic of NASA's Transparent Directional Solidification Furnace (TDSF).

Ampoules containing pure SCN and a SCN-1.0 mol.% (0.727 wt.%) ACE alloy were used in this study. The ampoules were filled and sealed under vacuum conditions. For the ampoule containing pure SCN, the material was first purified to eliminate any spurious solutal convection, and then 63-90 μm diameter porous SiO_2 seed particles were added. These seed particles are used to observe the convective flow in the melt. For the alloy ampoule, the SCN was first purified and then a specific amount of acetone added (again under vacuum) to achieve the desired concentration level.

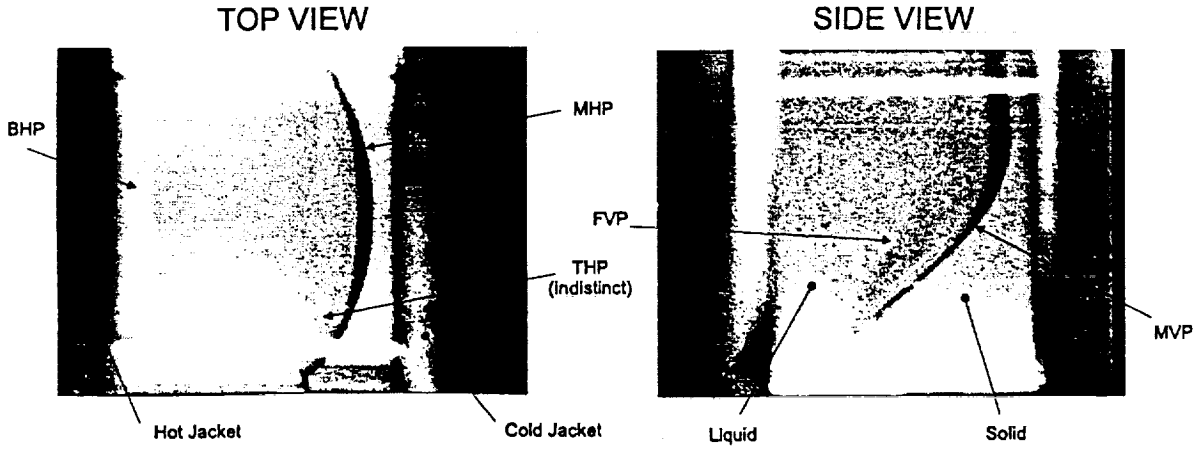

Figure 2. Sample of the images used to measure the solid/liquid interface positions. These images show the interface in (left) the x-z and (right) y-z planes.

Interface positions were determined by analyzing images of the interface captured from CCD video cameras, samples of which are shown in figure 2. The captured images were examined using image

processing software. In some cases, rudimentary image filtering was employed to enhance the edges of the interface. The scale of the image was determined using the distance between the hot and cold furnace on the image (which is known to be 5 mm on the apparatus). The primary sources of experimental error were uncertainties in the exact position of the interfaces, and uncertainties in determining the locations of the edges of the hot and cold furnaces, in the digital image. The experimental error in interface locations is estimated to be ± 0.2 mm. Since the system is assumed to be symmetric about the (y, z, 0) plane, interfaces in x-z planes (top view) are averaged to produce symmetric results [1]. Both the raw and averaged data are provided.

Thermal boundary conditions on the outside of the ampoule were measured in increments of 1 mm using K-type thermocouples glued on the exterior. A discussion of the experimental details of temperature measurement as well as the results are available in [1, 8]. The experimental error involved in locating the thermocouples is estimated to be ±0.2 mm. This error along with the finite thermal conductivity of the epoxies used for bonding and inherent thermocouple variability result in an estimated uncertainty of ±1 °C in the temperature readings. For the no growth experiments, the cold and hot zone temperature set points were 12 and 75 °C respectively, with an adiabatic zone length of 5 mm. For the 2 μm/s growth experiments a steeper thermal gradient was applied — the set points were 6 and 85 °C with an adiabatic zone length of 1 mm.

Pure Material (SCN) Results

Interface shapes under no-growth conditions are shown in figure 3. Figure 3(a) details the front shapes in y-z (vertical) planes. The acronym MVP refers to the "mid vertical plane", which is the vertical plane running along the longitudinal centerline of the ampoule (0, y, z); FVP refers to the "front vertical plane", which is the vertical plane running along the inside of the front wall of the ampoule (3, y, z). The interface shape at the FVP should be identical to that at the rear vertical plane (-3, y, z) from symmetry. Note that the interface is considerably distorted from the vertical, with the solid forming a concave shape. The maximum deflection of the interface occurs along the MVP. The interface in this plane extends from a position of (0, -3, 2.09) to (0, 1.46, -2.00) – a total displacement of 4.02 mm. The FVP is not as severely deflected from the vertical as the MVP, ranging from (0, -3, 2.09) to (0, 2.92, -0.76). Figure 3(b) is a plot of the front shapes in x-z (horizontal) planes. The acronym MHP refers to the "mid horizontal plane", which is the horizontal plane through the height at which maximum interface deflection occurs (x, ~1.6, z). BHP and THP refer to the horizontal planes running along the inside of the bottom and top ampoule walls respectively (x, -3, z) and (x, 3, z). The interface shapes in the MHP and THP are crescent-shaped, with the solid side being concave. There is slight asymmetry in the results, with the MHP interface meeting the front wall at (-3, 1.5, -0.95) but the rear wall at (3, 1.5, -0.99). This would tend to indicate that the ampoule was slightly misaligned such that the rear wall was closer to the furnace than the front wall. An interesting feature of figure 3(b) is the interface shape at the BHP. The interface meets the bottom wall at an acute angle and the contact line is difficult to quantify. Under ideal conditions this line should be symmetric since ideal thermal boundary conditions are both symmetric and steady. Observations during the course of this investigation have shown the shape of the interface at the BHP to be very sensitive to thermal conditions – the shape can often slowly oscillate back and forth even if the remainder of the interface appears to be at steady state. As shown in figure 3(b), the interface in the BHP is not symmetric but is melted back closer to the rear wall, providing further evidence that the ampoule was slightly misaligned. Quantitative measurements of the interface shape at the BHP could not be determined in [1]. The distorted interface shapes indicate that convection in the melt region has a significant impact on thermal transport in the domain.

Interface locations for the 40 μm/s growth case are shown in figure 4. Figure 4(a) is a plot of the interface shapes in the MVP and FVP. As compared to the no-growth case, the interface has become much more elongated but has retained the same general shape. The location of the interface near the bottom wall is (0, -3.00, 0.17), while the point of maximum deflection is (0, 1.22, -6.92) – a total deflection of 7.09 mm, compared with 4.02 mm for the no-growth case. Considering the interfaces in the FVP and the MVP, the separation between the interfaces in the FVP and MVP is larger than for the no-growth case. Figure 4(b) is a plot of the interface shape in the horizontal mid plane (x, 1.5, z). Once again, this front is crescent shaped as in the no-growth case but is much more concave, with a smaller minimum radius of curvature. Interface locations in the other planes could not be determined quantitatively due to inadequate clarity of the CCD video images. The imposition of translating boundary conditions has led to the interface being much more distorted than for the no-growth case (refer to figure 3). Interface locations for 2 μm/s growth conditions are quite similar to the no-growth case, and are available in [8].

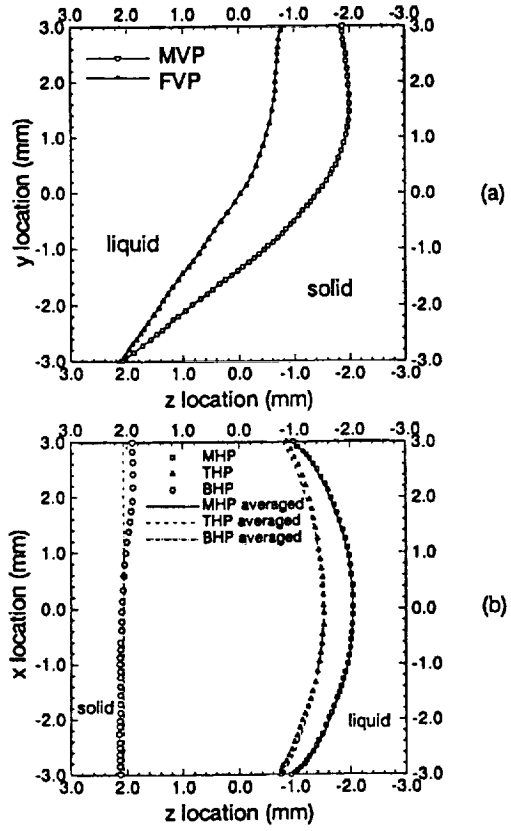

Figure 3. Front locations for pure SCN under no-growth conditions in (a) vertical planes and (b) horizontal planes.

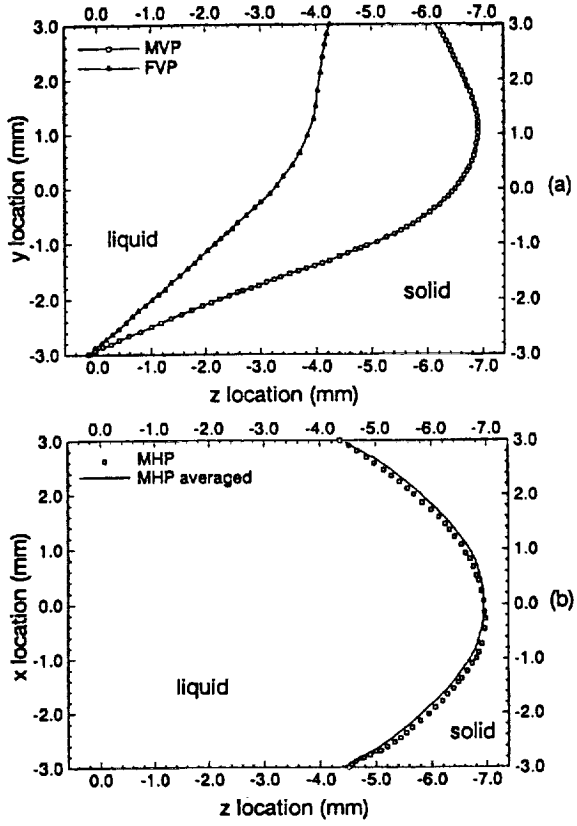

Figure 4. Front locations for pure SCN at a growth rate of 40 μm/s in (a) vertical planes and (b) horizontal planes. Translation of the furnaces has led to an elongation of the interface in z.

A comparison between the results shown in the present study and those in [1] for the no-growth and 40 μm/s cases yields the following comments. The majority of interface locations agree to within experimental error. For the more distinct and clearly defined interfaces (such as those in the MVP for the no-growth case), agreement was particularly good – often to within 0.05 mm. For some of the less distinct interfaces, agreement deteriorated. The maximum difference was observed to occur for some points near the ampoule walls for THP and MHP interfaces, with discrepancies of approximately 0.4 mm. This upper bound on the difference between results is due to the sensitivity of the interface to thermal boundary conditions and variability of each data set within the ±0.2 mm

range. Overall, agreement is good.

The motion of seed particles in the melt was filmed for a period of 10 minutes for the no-growth case. For the growth cases, particles near the interface were observed and filmed by sliding the cold furnace away from the interface zone to reveal the interface. This was done for time periods of a maximum of 40 seconds so as to minimize the impact of removing the cold furnace on the thermal condition on the outside of the ampoule, and hence, on the results. The interface was observed to continue at the normal growth rate for this length of time; if the cold zone is removed for any longer the interface movement begins to slow down appreciably, indicating that the thermal conditions have been appreciably changed.

A novel lighting condition was employed to reveal the particles while minimizing glare from surfaces and defects. This involved pointing two focused beams from fiber-optic light sources equipped with polarizing filters along the axis of the ampoule, one directed from outside the hot zone towards the cold zone and one located at the other end of the ampoule pointing toward the hot zone. In this way, the transparent ampoule and phase change material behaved like a "light pipe". Lighting conditions are crucial to the acquisition of acceptable video images of the seed particles; no other positions for the light sources yielded acceptable results.

The number density of particles in the melt was high, making flow visualization straightforward. The following general observations about the flow patterns in both the no-growth and growth cases can be made. Footage of the ampoule from the side (*i.e.* images of the y-z plane) reveals a single, longitudinal, primary convective cell. The flow moves along the top wall towards the interface; as it approaches the (cold) interface it is forced down and away from the interface in an arc shaped in a "reverse-C". The particle travel path near the interface resembles the shape of the interface itself. The fluid returns to the hot melt region by traveling along the bottom wall away from the interface. This general description of the flow is true for both the no-growth and growth cases. Particles that travel near the interface are clearly affected by the viscous layer and are noticeably slower. Occasionally, these particles would become entrained in the approaching front for the growth case. The velocity of particles traveling through the (x, y, z) point (0, +0.90, -1.30) was measured to be 1.46 ± 0.1 mm/s. Observations of the ampoule from above (*i.e.* images of the x-z plane) reveal only slight secondary flows present near the interface. These observations indicate that the convective flow is primarily a single two-dimensional cell in the y-z plane with secondary convective motions restricted to x-z planes near the interface.

Alloy (SCN-ACE) Results

The no-growth interface shapes for the alloy (available in [8]) are very similar to those for no-growth pure SCN, with the key difference being in the location of the interface. The lowest z location for the alloy interface is -3.67 mm, whereas the lowest z location for the pure SCN case is -2.00 mm. The change in position is clearly due to the decrease of the interface temperature caused by the addition of the acetone.

The 2 μm/s growth results for the alloy are shown in figure 5. As in the no-growth case, the MVP alloy interface shape has a shape which is very similar to the pure material case, while the values for the FVP interface are pushed slightly closer to the MVP results. This trend is confirmed from examining the interfaces in the horizontal planes (figure 5(b)). The maximum deflection for this case is 4.28 mm, compared with 4.68 mm for the no-growth alloy case.

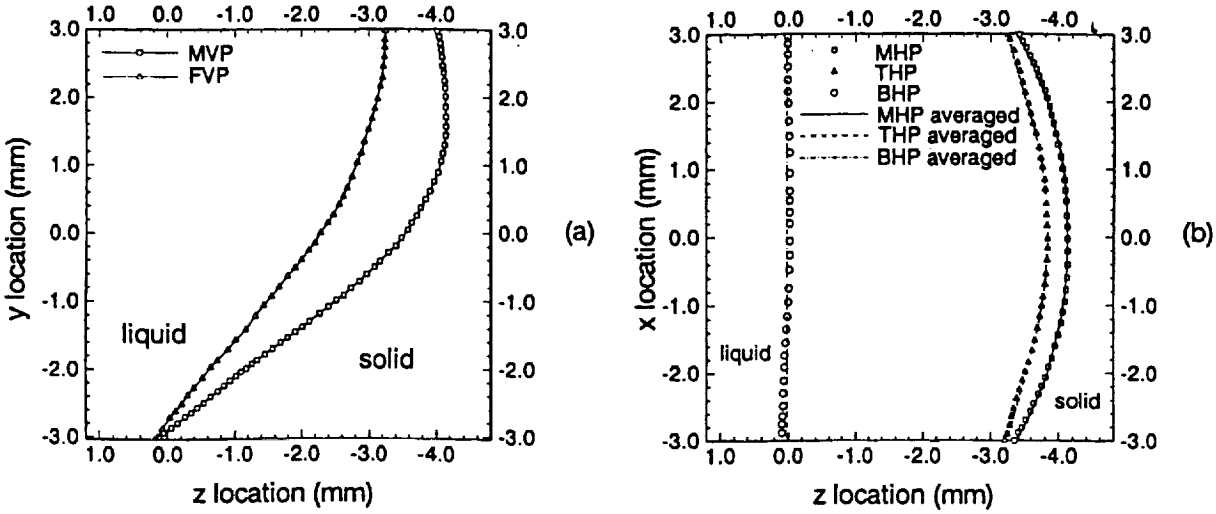

Figure 5. Front locations for SCN-ACE at a growth rate of 2 μm/s in (a) vertical planes and (b) horizontal planes. The temperature gradients near the interface have increased for this experiment, leading to a more compact interface shape even though the furnaces are translating.

Numerical Simulations

Two-dimensional numerical simulations for pure SCN and the SCN-ACE alloy under no-growth conditions were performed. The flow visualizations discussed above revealed that the convective flow is primarily 2D in nature; a 2D analysis is thus expected to be a good representation of the process. The solution scheme used is described in full in Simpson and Garimella [6]. Melt velocities are solved using a vorticity-stream function formulation of the momentum and continuity equations. The energy equation, incorporating phase-change, is solved using the enthalpy method which is a single-domain approach that does not require the front to be explicitly tracked. Conduction in the ampoule wall is incorporated in the solution scheme. The solution scheme has the capacity to model fully transient phase change processes and the effects of solute redistribution at the interface. For no-growth conditions for both the pure material and alloy, the heat and flow fields are at steady state; moreover, there are no compositional variations in the melt region for the alloy at steady state. The alloy was therefore treated as a pure material; species concentration was not considered.

Thermophysical properties were constant in both the solid and liquid phases but not equal. The property values used for pure SCN were obtained from reference [9]: $k_l = 0.223$ W/mK, $k_s = 0.225$ W/mK, $C_{pl} = 2000$ J/kgK, $C_{ps} = 1955$ J/kgK, $\rho = 990$ kg/m^3, $L = 46.24$ J/kg, $\beta_T = -8.1 \times 10^{-4}$ 1/K, $\mu = 3.0 \times 10^{-3}$ Ns/m, and a melting temperature of $T_m = 58.08$ °C. Properties for the borosilicate glass ampoule were obtained from [10]: $k_w = 1.2$ W/mK, $C_{pw} = 753.5$ J/kgK, $\rho_w = 2300$ kg/m^3. For the SCN-1.0 mol.% (0.727 wt.%) ACE alloy, thermophysical properties for pure SCN alloy are used but the melting temperature was altered. The slope of the liquidus line for the SCN-ACE system is $m = -2.8$ K/wt.% yielding a melting temperature of $T_m = 56.04$ °C. Terrestrial gravity of $g = 9.81$ m^2/s acts in the negative-y direction.

For the boundary conditions, no-growth temperature profiles from [1] are used for both the pure and alloy simulations. It is not necessary to model the entire 150 mm length of the ampoule. The simulation domain extends from $z = -19$ mm in the solid to +40 mm in the melt. Since there are only small temperature gradients further into the melt, numerical experiments have shown that

convective velocities are not substantially changed by lengthening the domain to z = +60 mm.

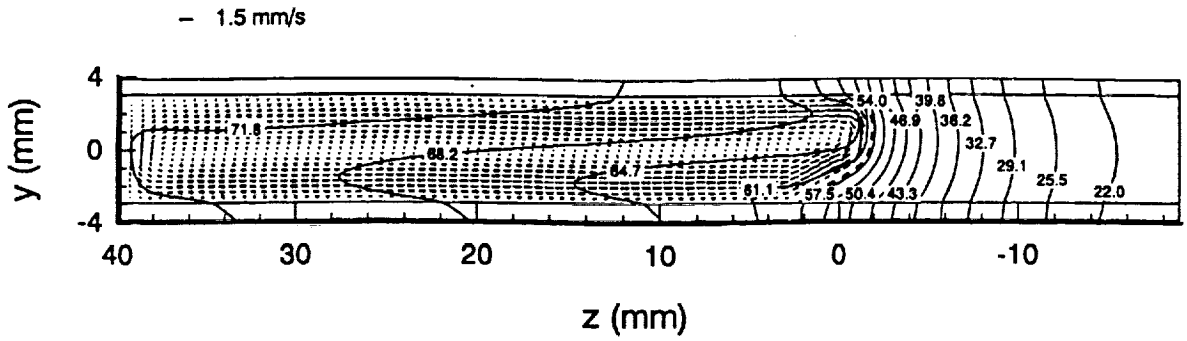

Figure 6. Plot of velocity vectors and isotherms from the numerical simulation for pure SCN under no growth. Velocity vectors are plotted at every second mesh point in the z-direction.

A 200 × 20 mesh was used for the results shown in this work. Simulations at a coarser 100 × 10 mesh have maximum convective velocities 10% smaller than those at the refined mesh. The CPU burden for each simulation was 5.6 hours on a DEC 300 MHz Alphaserver 2100A. Since the solution scheme is fully transient, steady-state solutions were obtained by solving the time-dependent problem until steady-state conditions are obtained.

Figure 6 is a plot of the velocity vectors and isotherms for the pure SCN case. The dashed line is the interface location. A single, clockwise rotating longitudinal convective cell formed in the SCN melt. Warm bulk fluid moves along the top wall and washes onto the top of the interface. The fluid then falls toward the bottom wall and is convected away. The interface takes on a distinctly curved shape with the solid being concave. This shape is due to the influence of convection on the interface shape; warm fluid introduced to the interface near the top wall acts to melt the interface back. As the fluid cools and falls toward the bottom wall the interface is distorted less. The maximum convective velocity was found to be 1.515 mm/s at the location (z, y) of (−1.30, +0.90), which is near the interface where applied temperature gradients are steepest. This value agrees well with the experimentally estimated value of 1.46 ± 0.1 mm/s in the same location. Note also the influence of the ampoule walls on the process; the difference between the temperatures on the inside and outside of the walls is largest near the interface. At z = 0 the temperature differences are 2.14 K and 1.23 K for the top and bottom walls, respectively.

Figure 7(a) is a comparison of experimentally and numerically determined interface locations. Two sets of experimentally determined interface shapes are included on this plot, both those from [1] and those measured in this work. The calculated and measured interface shapes agree to within a maximum discrepancy of 0.47 mm, with over half of the results exhibiting a maximum discrepancy of 0.25 mm. This is acceptable agreement given the variability of the measured temperature boundary conditions (±1K) and the experimental error in determining the interface of ±0.2 mm. Other finite element and finite-difference simulations of the same process [10, 11, 12] exhibit maximum discrepancies of 0.30 to 0.45 mm.

Velocity vectors and isotherms for the SCN-ACE alloy case are similar to those for pure SCN and are not shown. The maximum convective velocity is 1.724 mm/s at a location (z, y) of (−2.18, 0.90). This value is slightly larger than that found for the pure case and is a consequence of the lower melting temperature increasing the driving force for convection. Figure 7(b) is a comparison of experimentally and numerically determined interface locations for the alloy. The results agree to within 0.3 mm for the lower half of the domain, however, agreement is poor (a maximum

discrepancy of 1.4 mm) in the top half of the domain. Investigation of the temperatures applied at the top boundary reveals that the temperature applied at the z location where the interface meets the top wall (-3.48 mm) is 47.7°C, well below the alloy interface temperature of 56.04°C. For the case shown in figure 7(a) the applied temperature is 57°C which is close to the interface temperature (58.08 °C). This suggests that the top wall temperature profile for the alloy ampoule is slightly different to that measured for the pure SCN case (recall that the pure SCN boundary condition is used for both the pure and alloy simulations). A more accurate boundary condition needs to be sought in order to faithfully simulate the process (possibly by translating the pure SCN temperature boundary condition so that the applied temperature is ~56.04°C at z = -3.48 mm).

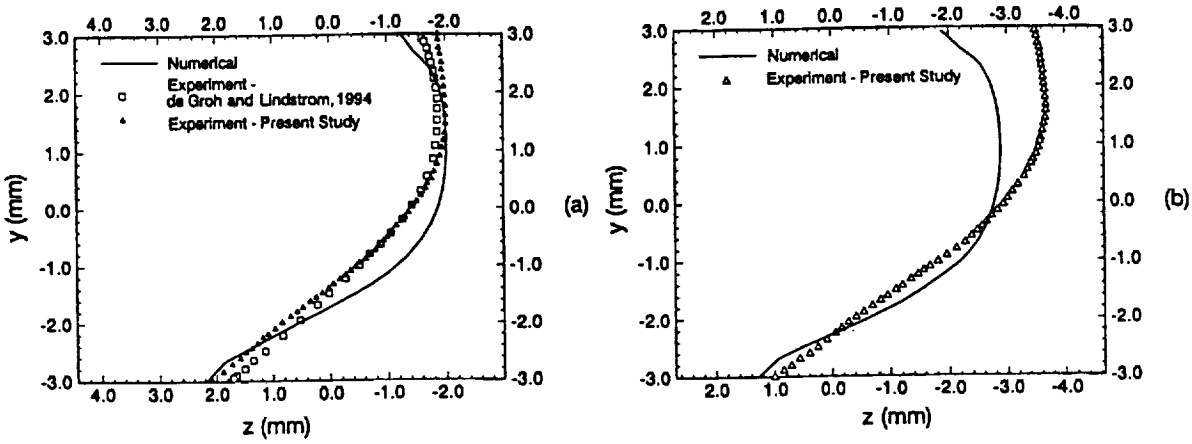

Figure 7. Comparison of experimentally and numerically determined interface locations during no-growth for (a) pure SCN, and (b) SCN-1.0 mol% ACE.

Conclusions

The horizontal Bridgman crystal growth of pure SCN and a SCN-1.0 mol.% ACE alloy has been experimentally investigated. Interface shapes obtained for pure SCN agree reasonably well with data found in a previous study [1]. The interface shapes for pure SCN are stable and non-dendritic; however they are not flat but instead assume a complex three-dimensional shape. This indicates the presence of thermally driven convective motion in the melt region which influences the interface shape.

Flow visualization using digital video images indicates that a single longitudinal convective cell forms, with warm fluid approaching the interface from the top of the domain, falling at the cool interface and retreating along the bottom of the ampoule. This cell is primarily two-dimensional – the only secondary flows observed occur near the interface and act to push approaching fluid out from the centerline toward the side walls. The convective velocity at a location (x, y, z) of (0, +0.90, -1.30) for the no-growth case has been measured from the flow visualization to be 1.46 ± 0.1 mm/s.

Interface shapes for the alloy appear to be similar in nature to those determined for the same conditions using pure SCN and so are influenced by thermally driven convection. The interfaces occur at lower temperatures than for the pure SCN case. This is a result of the reduction of the interface temperature due to the introduction of the solute. Growth of the alloy was experimentally found to be unstable and dendritic for growth velocities above 2.8 μm/s.

Numerical simulations of both the pure SCN and SCN-ACE alloy no-growth cases confirm the role of convection in influencing the interface shape. For the pure SCN case, a single longitudinal

convective cell is formed. The introduction of warm bulk fluid to the interface melts the interface back and imparts the characteristic distorted shape. The numerical results exhibit acceptable agreement with the experiment; the calculated interface shape lies within 0.47 mm of the measured location and the maximum velocity of 1.515 mm/s is similar to the experimental value in the same location of 1.46 ± 0.1 mm/s. For the simulation of the SCN-ACE case the agreement between the calculated and measured interface shape is poor in the top half of the ampoule. This indicates that a more appropriate thermal boundary condition along the top wall for the alloy ampoule needs to be determined.

In ongoing work, fully transient simulations of growth cases of the pure material and alloy (including solute redistribution at the interface) are being carried out.

G. de Vahl Davis, E. Leonardi and V. Timchenko of University of New South Wales are thanked for kindly providing their code FRECON3V, which was the starting point for the numerical code used in this work.

References

1. H. C. de Groh III and T. Lindstrom, "Interface Shape and Convection During Solidification and Melting of Succinonitrile" (NASA Technical Memorandum 106487, June 1994).

2. S. V. Garimella, J. P. McNulty and L. Z. Schlitz, "Formation and Suppression of Channels during Upward Solidification of a Binary Mixture," *Metall. and Mater. Trans.*, 26A (1995), 971-981.

3. C. S. Magirl and F. P. Incropera, "Flow and Morphological Conditions Associated with Unidirectional Solidification of Aqueous Ammonium Chloride" (ASME HTD-Vol. 206, 1992), 1-9.

4. P. M. Adornato and R. A. Brown, "Convection and Segregation in Directional Solidification of Dilute and Non-Dilute Binary Alloys: Effects of Ampoule and Furnace Design," *J. Crystal Growth*, 80 (1987), 155-190.

5. M. C. Liang and C. W. Lan, "Three-Dimensional Convection and Solute Segregation in Vertical Bridgman Crystal Growth," *J. Crystal Growth*, 167 (1996), 320-332.

6. J. E. Simpson and S. V. Garimella, "An Investigation of the Solutal, Thermal and Flow Fields in Unidirectional Alloy Solidification," *Int. J. Heat Mass Transfer*, 41 (1998), 2485-2502.

7. X. Zeng and A. Faghri, "Temperature-Transforming Model for Binary Solid-Liquid Phase-Change Problems, Part II: Numerical Simulation," *Numer. Heat Transfer B*, 25 (1994), 481-500.

8. J. E. Simpson et al., "Directional Solidification of Pure Succinonitrile and a Succinonitrile-Acetone Alloy" (NASA Technical Memorandum, in review).

9. C. J. Paradies, "The Influence of Forced Convection during Solidification on Fragmentation of the Mushy Zone of a Casting" (Ph.D. thesis, Rensselaer Polytechnic Institute, 1993).

10. H. C. de Groh III and M. Yao, "Numerical and Experimental Study of Transport Phenomena in Directional Solidification of Succinonitrile" (ASME HTD-Vol. 284, 1994), 227-243.

11. G. H. Yeoh et al., "A Numerical and Experimental Study of natural Convection and Interface Shape in Crystal Growth," *J. Crystal Growth*, 173 (1997), 492-502.

12. P. Y. P. Chen et al., "A Numerical Study of Directional Solidification and Melting in Microgravity"(Procs. IMECE, Anaheim, CA, 1998).